Heavy Quark Treatment

Robert Thorne

August 23rd, 2011

University College London

Associate of IPPP Durham

Will discuss Charm $\sim 1.5\mathrm{GeV}$, bottom $\sim 4.3\mathrm{GeV}$, and at end strange $\sim 0.3\mathrm{GeV}$ as heavy flavours.

Two distinct regimes:

Near threshold $Q^2 \sim m_H^2$ massive quarks not partons. Created in final state. Described using **Fixed Flavour Number Scheme** (FFNS).

$$F(x,Q^2) = C_k^{FF,n_f}(Q^2/m_H^2) \otimes f_k^{n_f}(Q^2)$$

Note that n_f is effective number of light quarks. Can be $3, 4$ or 5.

Does not sum $\alpha_S^n \ln^n Q^2/m_H^2$ terms in perturbative expansion. Usually achieved by definition of heavy flavour parton distributions and solution of evolution equations.

Additional problem FFNS known up to NLO (Laenen et al), but are not defined at NNLO – $\alpha_S^3 C_{2,Hg}^{FF,3}$ not fully known (see talk by Blümlein).

Variable Flavour

High scales $Q^2 \gg m_H^2$ massless partons. Behave like up, down (strange always in this regime. Sum $\ln(Q^2/m_H^2)$ terms via evolution. **Zero Mass Variable Flavour Number Scheme** (ZM-VFNS). Ignores $\mathcal{O}(m_H^2/Q^2)$ corrections.

$$F(x,Q^2) = C_j^{ZM,n_f} \otimes f_j^{n_f}(Q^2).$$

Partons in different number regions related to each other perturbatively.

$$f_j^{n_f+1}(Q^2) = A_{jk}(Q^2/m_H^2) \otimes f_k^{n_f}(Q^2),$$

Perturbative matrix elements $A_{jk}(Q^2/m_H^2)$ (Buza et al) containing $\ln(Q^2/m_H^2)$ terms relate $f_i^{n_f}(Q^2)$ and $f_i^{n_f+1}(Q^2) \rightarrow$ correct evolution for both.

Want a **General-Mass Variable Flavour Number Scheme** (VFNS) taking one from the two well-defined limits of $Q^2 \leq m_H^2$ and $Q^2 \gg m_H^2$.

Extrapolation between the two simple kinematic regimes for xF_3 measured using neutrino scattering at NuTeV.

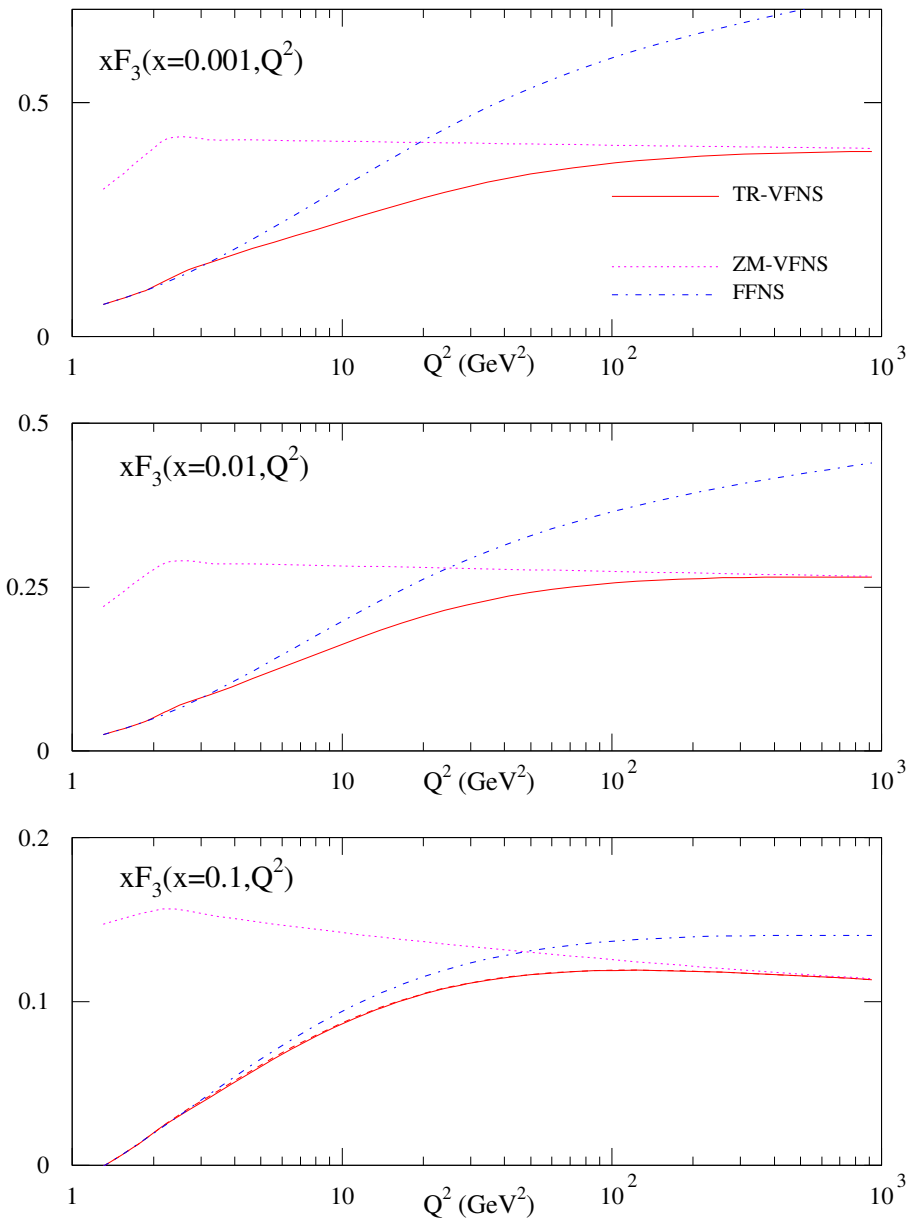

At NLO the partons remain continuous if transition point is taken as $Q^2 = m_H^2$. ZM-VFNS possible, if inaccurate.

At NNLO lead to discontinuities in partons.

Heavy flavour no longer turns on from zero at $\mu^2 = m_c^2$

$$(c + \bar{c})(x, m_c^2) = A_{Hg}^2(m_c^2) \otimes g(m_c^2)$$

In practice turns on from negative value, (for general gluon).

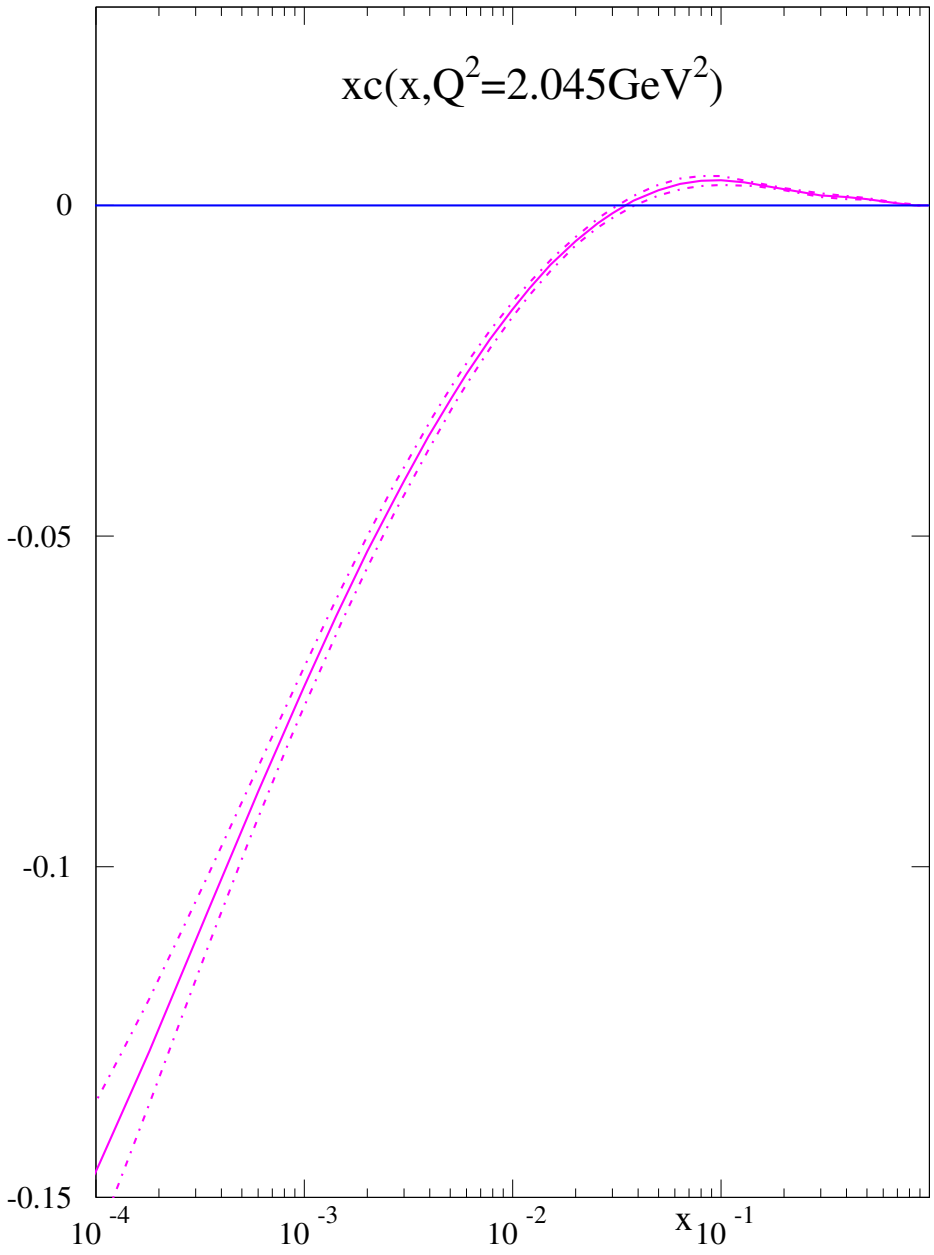

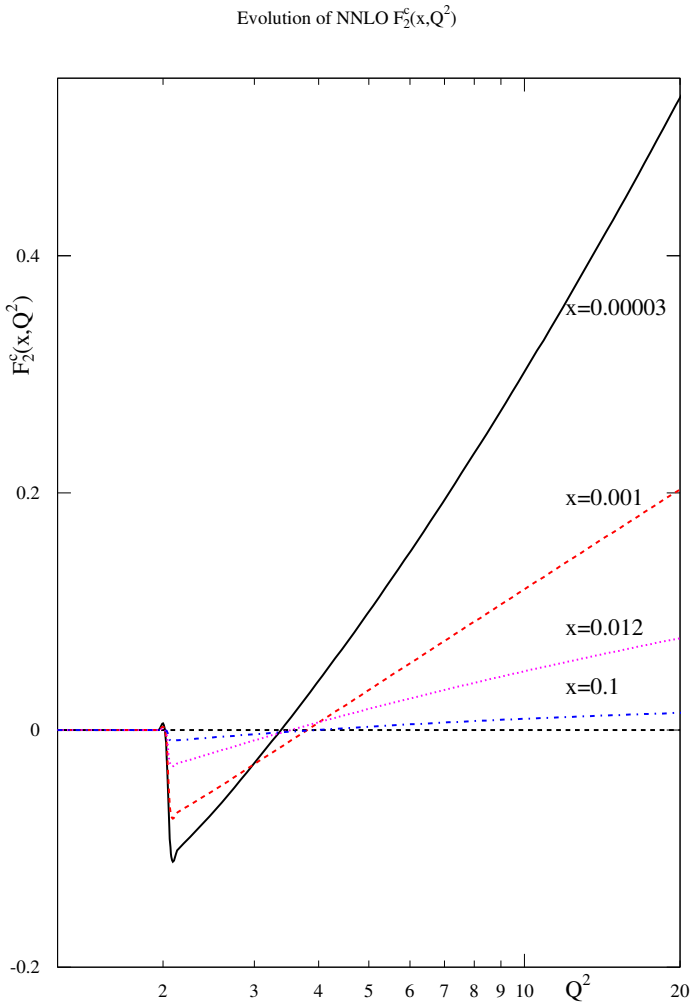

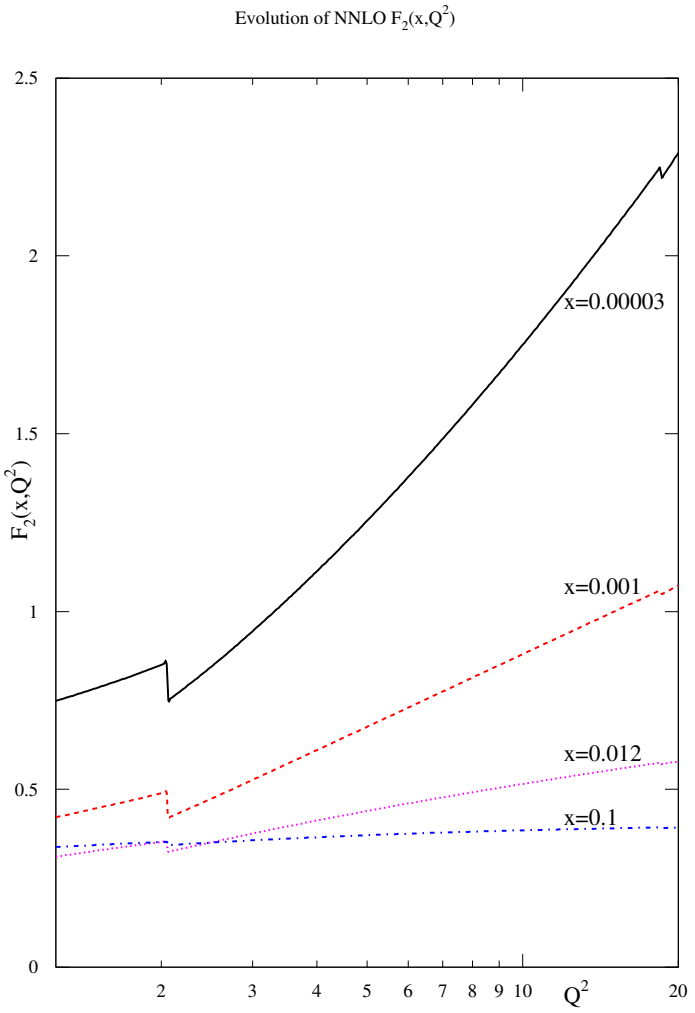

Leads to huge discontinuity in $F_2^c(x, Q^2)$. Still significant in $F_2^{Tot}(x, Q^2)$.

ZM-VFNS not really feasible at NNLO. Want $\rightarrow$ Need.

The GM-VFNS can be defined by demanding equivalence of the n_f light flavour and n_f+1 light flavour descriptions at all orders – above transition point $n_f \to n_f+1$

$$F(x,Q^2) = C_k^{FF,n_f}(Q^2/m_H^2) \otimes f_k^{n_f}(Q^2) = C_j^{VF,n_f+1}(Q^2/m_H^2) \otimes f_j^{n_f+1}(Q^2)$$
$$\equiv C_j^{VF,n_f+1}(Q^2/m_H^2) \otimes A_{jk}(Q^2/m_H^2) \otimes f_k^{n_f}(Q^2).$$

Hence, the VFNS coefficient functions satisfy

$$C_k^{FF,n_f}(Q^2/m_H^2) = C_j^{VF,n_f+1}(Q^2/m_H^2) \otimes A_{jk}(Q^2/m_H^2),$$

which at $\mathcal{O}(\alpha_S)$ gives

$$C_{2,Hg}^{FF,n_f,(1)}(\frac{Q^2}{m_H^2}) = C_{2,HH}^{VF,n_f+1,(0)}(\frac{Q^2}{m_H^2}) \otimes P_{qg}^0 \ln(Q^2/m_H^2) + C_{2,Hg}^{VF,n_f+1,(1)}(\frac{Q^2}{m_H^2}),$$

The VFNS coefficient functions tend to the massless limits as $Q^2/m_H^2 \to \infty$.

However, $C_j^{VF}(Q^2/m_H^2)$ only uniquely defined in this limit.

Can swap $\mathcal{O}(m_H^2/Q^2)$ terms between $C_{2,HH}^{VF,0}(Q^2/m_H^2)$ and $C_{2,g}^{VF,1}(Q^2/m_H^2)$.

Various prescriptions (ACOT, TR, Chuvakin-Smith).

Some earlier versions violated threshold $W^2 > 4m_H^2$ in individual terms.

(TR-VFNS) highlighted freedom in choice and enforced kinematics in each term by making $(d\,F_2/d\,\ln Q^2)$ continuous at transition (in gluon sector). Complicated to extend.

(S)ACOT(χ) (Tung, *et al*) prescription says make simple choice

$$C_{2,HH}^{VF,0}(Q^2/m_H^2, z) \propto \delta(z - Q^2/(Q^2 + 4m_H^2)).$$

$$\rightarrow F_2^{H,0}(x, Q^2) \propto (h + \bar{h})(x/x_{max}, Q^2), \qquad x_{max} = Q^2/(Q^2 + 4m_H^2)$$

$\rightarrow C_{2,HH}^{ZM,0}(z) = \delta(1 - z)$ for $Q^2/m_H^2 \rightarrow \infty$. Also $W^2 = Q^2(1 - x)/x \geq 4m_H^2$.

Have adopted this and obvious extensions to higher orders (and now simple modifications). Though with different prefactor – chosen by analogy to $F_2^{\rm CC}$.

Still another difference.

ACOT type schemes have used e.g.

NLO $\quad \frac{\alpha_S}{4\pi} C_{2,Hg}^{FF,n_f,(1)} \otimes g^{n_f} \rightarrow \frac{\alpha_S}{4\pi} (C_{2,HH}^{VF,n_f+1,(1)} \otimes (h+\bar{h}) + C_{2,Hg}^{VF,n_f+1,(1)} \otimes g^{n_f+1})$,

i.e., same order of α_S above and below.

But LO FFNS and evolution below and NLO definition and evolution above.

TR have used e.g.

LO $\quad \frac{\alpha_S(Q^2)}{4\pi} C_{2,Hg}^{FF,n_f,(1)}(Q^2/m_H^2) \otimes g^{n_f}(Q^2) \rightarrow \frac{\alpha_S(M^2)}{4\pi} C_{2,Hg}^{FF,n_f,(1)}(1) \otimes g^{n_f}(M^2)$

$$+C_{2,HH}^{VF,n_f+1,(0)}(Q^2/m_H^2) \otimes (h+\bar{h})(Q^2),$$

i.e. freeze higher order α_S term when going upwards through $Q^2 = m_H^2$.

This difference in choice can be phenomenologically important.

In order to define our VFNS at NNLO, need $\mathcal{O}(\alpha_S^3)$ heavy flavour coefficient functions for $Q^2 \leq m_H^2$ and to be frozen for $Q^2 > m_H^2$. However, not calculated. Needs modelling. More later.

Remember caveat at NNLO. At NNLO also get contribution due to heavy flavours away from photon vertex.

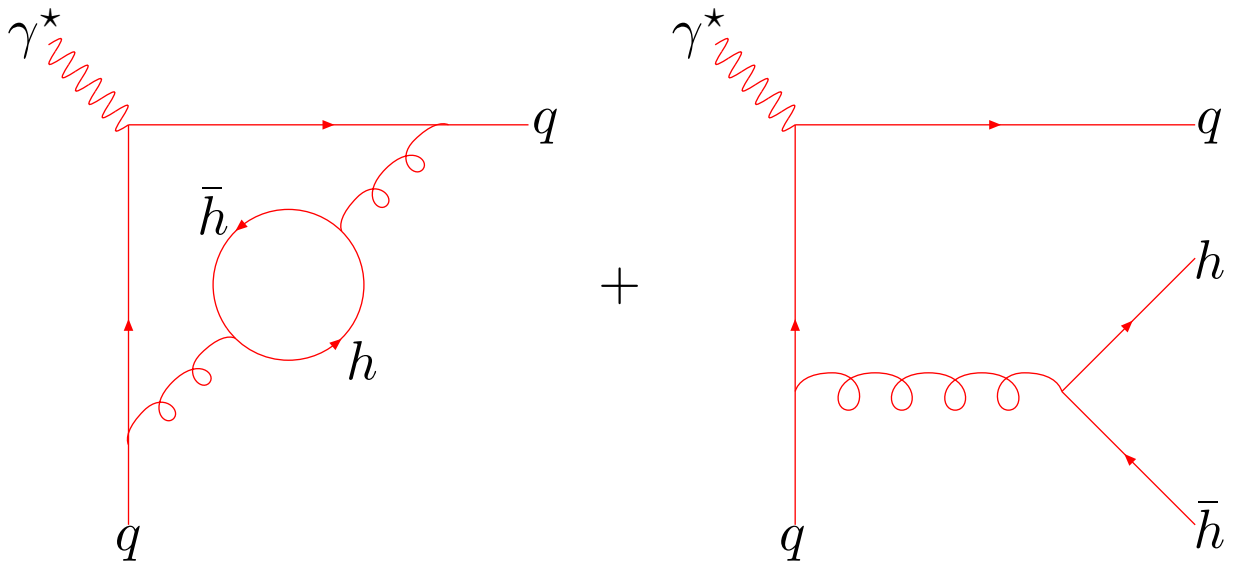

Strictly, left-hand type diagram and soft parts of right-hand type diagram should be light flavour structure function, and hard part of right-hand type diagram contributes to $F_2^H(x, Q^2)$ (Chuvakin, Smith, van Neerven).

Soft part of right cancels $\ln^3(Q^2/m_H^2)$ divergences in virtual corrections (left).

Can be implemented (depends on separation parameter), but each contribution tiny. At moment all in light flavours. Not so small if $\ln^3(Q^2/m_H^2)$ terms not cancelled.

NNLO consequences (2006).

NNLO $F_2^c(x, Q^2)$ starts from higher value at low Q^2.

At high Q^2 dominated by $(c + \bar{c})(x, Q^2)$. This has started evolving from negative value at $Q^2 = m_c^2$. Remains lower than at NLO for similar evolution.

General trend – $F_2^c(x, Q^2)$ flatter in Q^2 at NNLO than at NLO. Important effect on gluon distribution going from one to other.

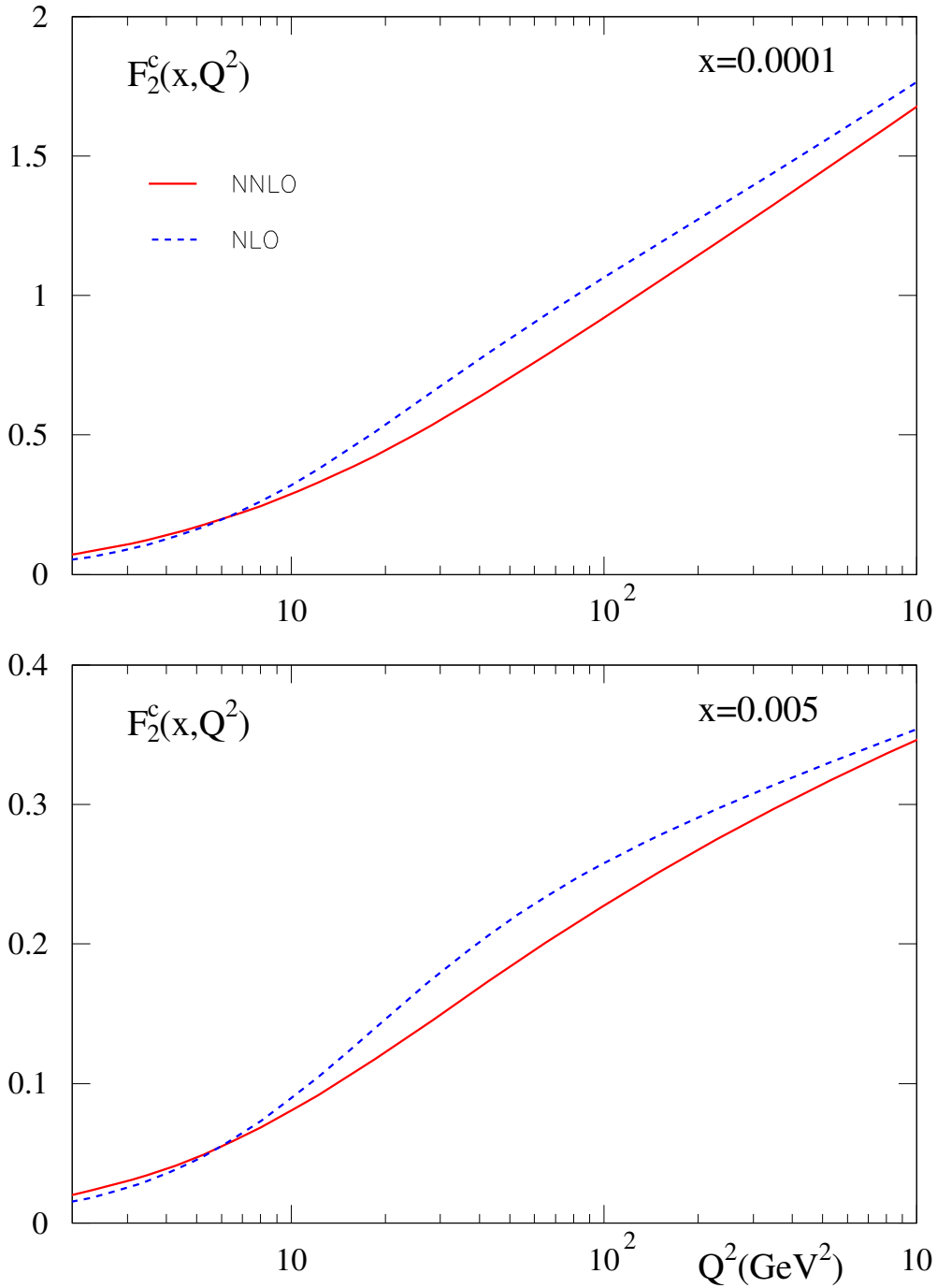

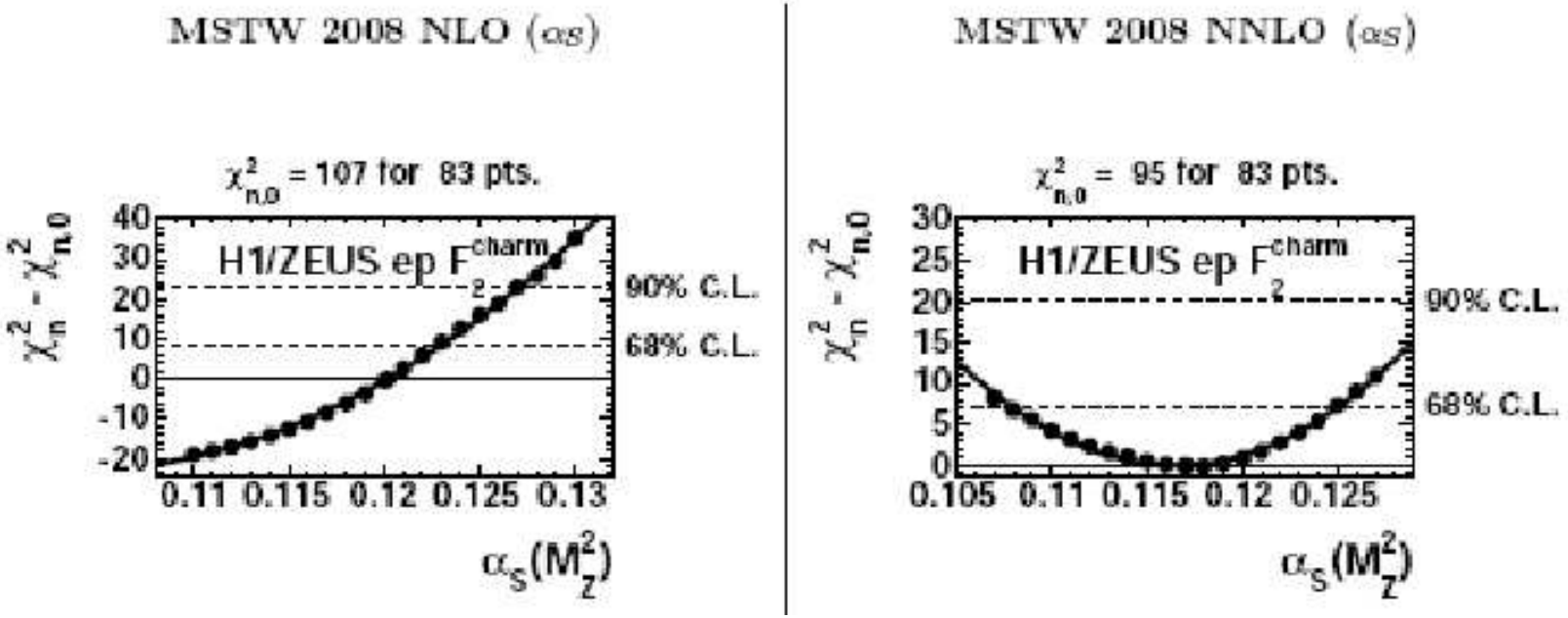

The $\Delta\chi^2$ profile is stabilised by NNLO corrections.

HERA $F_2^{c\bar{c}}(x, Q^2)$ data prefer slope predicted at NNLO – difficult to achieve at NLO.

Different type of Definition

Both the BMSN (Buza *et al*) and FONLL (Nason *et al*) applied the same type of reasoning in initially different contexts. In general terms (for structure functions)

$$F^{\rm GMVFNS}(x,Q^2) = F_2^{\rm FFNS}(x,Q^2) - F_2^{\rm asymp}(x,Q^2) + F_2^{\rm ZMVFNS}(x,Q^2)$$

where the second (subtraction) term is the asymptotic version of the first, i.e., all terms $\mathcal{O}(m_H^2/Q^2)$ omitted.

Differences in exactly how the second and third terms are defined in detail (e.g. Blümlein *et al* do not resum $\ln Q^2/m_H^2$ terms from PDF evolution in $F_2^{\rm ZMVFNS}$).

Question of whether one only uses above some transition point, else not exactly $F_2^{\rm FFNS}(x,Q^2)$ below $Q^2 = m_H^2$.

Realised from the beginning in FONLL approach that each term in the combination $(F_2^{\rm ZMVFNS} - F_2^{\rm asymp})$ can be modified by corrections which fall like m_H^2/Q^2.

In simplest application α_S order of $F^{\rm FFNS}(x,Q^2)$ at low Q^2 same as that of $F^{\rm ZMVFNS}(x,Q^2)$ as $Q^2 \to \infty$, like ACOT.

Modification in FONLL (Forte *et al*) can avoid this, but leads to extra (higher order) term as $Q^2 \to \infty$ – not exact cancellation in first two terms.

Ordering tricky problem. Would like any GMVFNS to reduce to exactly correct order FFNS at low Q^2 and exactly correct order ZMVFNS as $Q^2 \to \infty$. At present none do.

Return to particular TR version of the GMVFNS. Reason for violation of the above is frozen term $\alpha_S^n(m_H^2)\sum_i C_{2,i}^{\rm FFNS}(m_H^2)\otimes f_i(m_H^2)$ which still persists as $Q^2 \to \infty$ at order $\mathrm{N}^{n-1}\mathrm{LO}$.

Depends on size of PDFs at low scales, so rather small effect at large Q^2.

However, not strictly necessary. Frozen in original TR prescription from exact condition on derivative of $d\,F_2/d,\ln Q^2$. Could have instead

$$\left(\frac{m_H^2}{Q^2}\right)^a \alpha_S^n(m_H^2)\sum_i C_{2,i}^{\rm FF}(m_H^2)\otimes f_i(m_H^2) \text{ or } \left(\frac{m_H^2}{Q^2}\right)^a \alpha_S^n(Q^2)\sum_i C_{2,i}^{\rm FF}(Q^2)\otimes f_i(Q^2),$$

Any $a > 0$ provides both exactly correct asymptotic limits, though strictly should have $(m_H^2/Q^2)k\big(\ln(Q^2/m_H^2)\big)$ from factorization theorem.

Also have the freedom to modify the heavy quark coefficient function, by default

$$C_{2,HH}^{VF,0}(Q^2/m_H^2, z) = \delta(z - x_{\max}).$$

Appears in convolutions for higher order subtraction terms, so do not want complicated x dependence. Simple choice.

$$C_{2,HH}^{VF,0}(Q^2/m_H^2, z) \to (1 + b(m_H^2/Q^2)^c)\delta(z - x_{\max})),$$

where again c really encompasses (m_H^2/Q^2) with logarithmic corrections.

Can also modify argument of δ-function, as in Intermediate Mass (IM) scheme of Nadolsky, Tung. Let argument of heavy quark contribution change like

$$\xi = x/x_{\max} \to x\big(1 + (x(1 + 4m_H^2/Q^2))^d 4m_H^2/Q^2\big),$$

so kinematic limit stays the same, but if $d > 0$ small x less suppressed, or if $d < 0$ (must be > -1) small x more suppressed.

Default a, b, c, d all zero. Limit either by fit quality or *sensible* choices.

6 extreme variations tried.

GMVFNS1 – $b = -1, c = 1$.

GMVFNS2 – $b = -1, c = 0.5$.

GMVFNS1 – $a = 1$.

GMVFNS1 – $b = +0.3, c = 1$ – fit.

GMVFNS1 – $d = 0.1$ – fit.

GMVFNS1 – $d = -0.2$ – fit.

Variations in $F_2^c(x, Q^2)$ near the transition point at NLO due to different choices of GM-VFNS.

Optimal, $a = 1, b = -2/3, c = 1$, smooth behaviour.

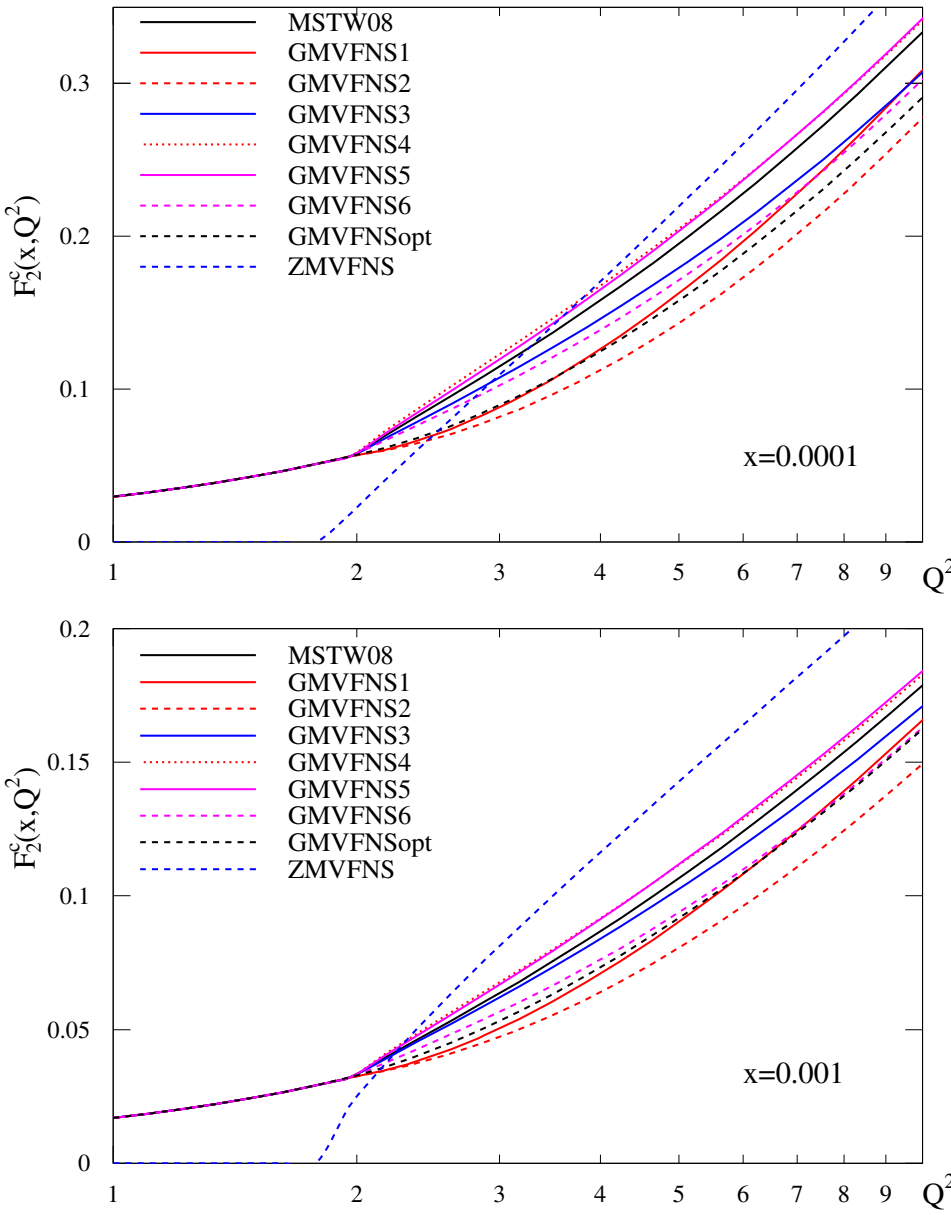

Variations in $F_2^c(x, Q^2)$ near the transition point due to different choices of GM-VFNS at NNLO.

Very much reduced, almost zero variation until very small x.

Shows that NNLO evolution effects most important in this regime.

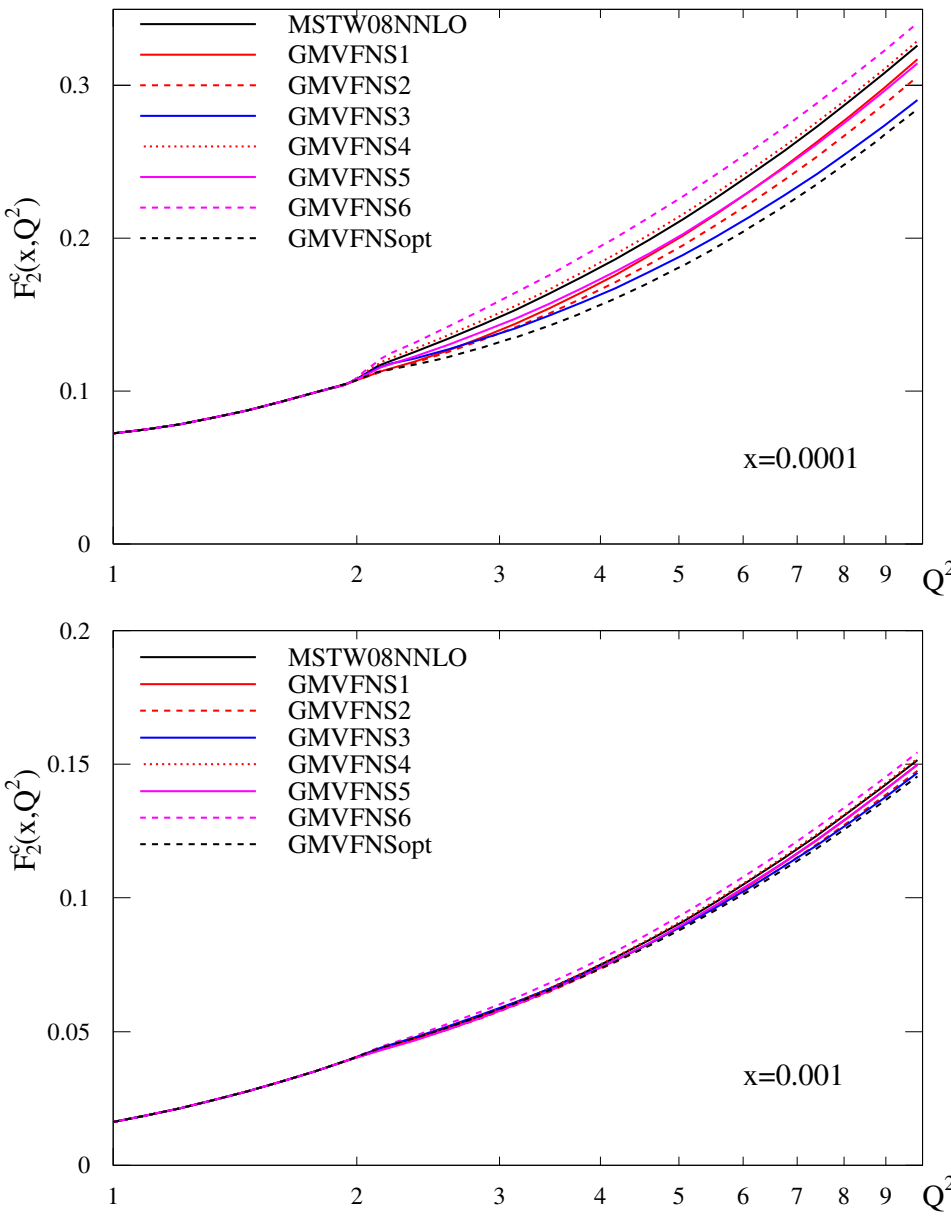

Variations in partons extracted from global fit due to different choices of GM-VFNS at NLO.

Initial χ^2 can change by 250.

Converges to at most about 15 of original.

Better fit for GMVFNS1, GMVFNS3 and GMVFNS6.

Some changes in PDFs large compared to one-sigma *uncertainty*.

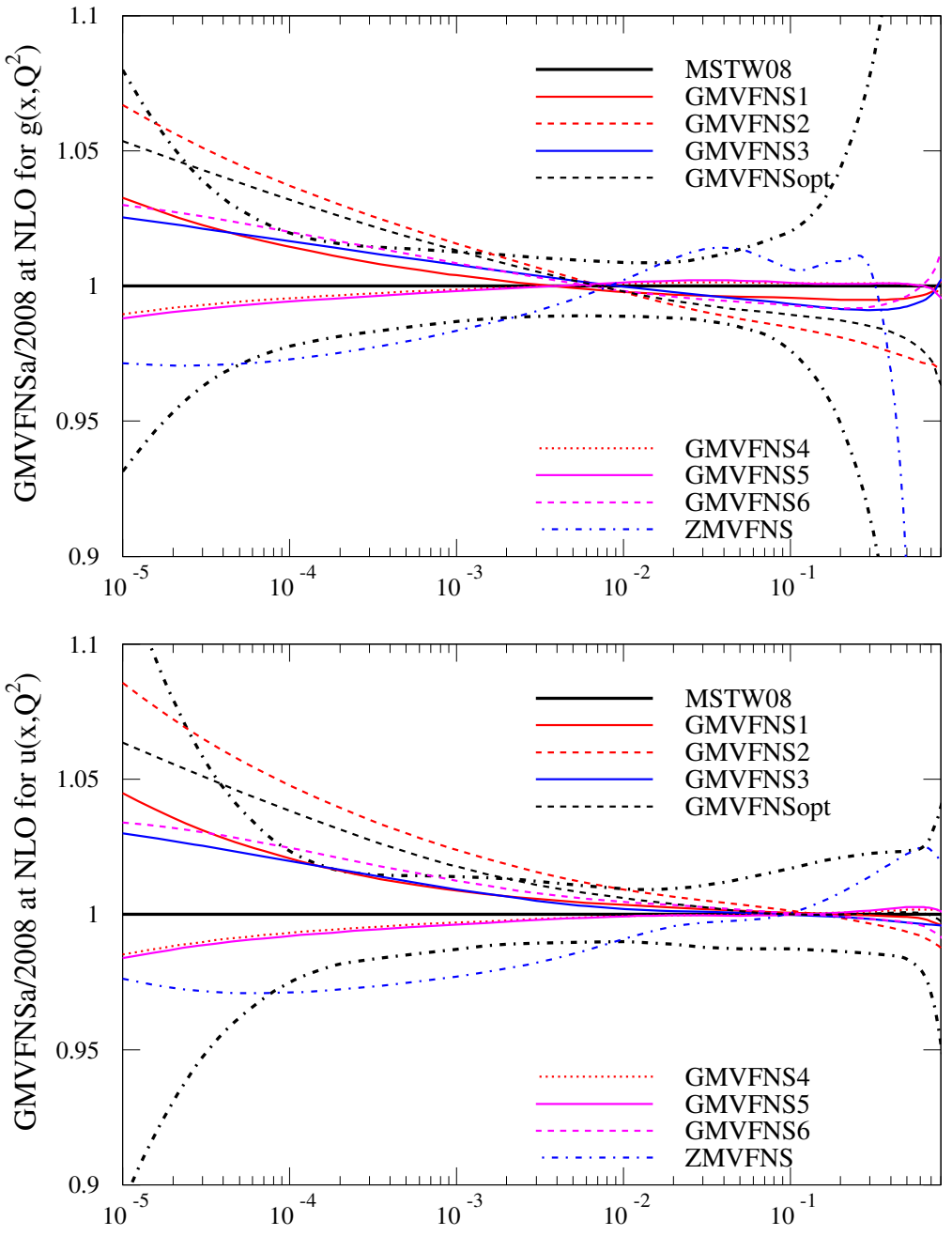

Also implement similar variations in GMVFNS for charged current processes.

HERA data completely insensitive due to large Q^2.

Some effect on fixed target (anti)neutrino data. χ^2 changes by at most 4 and almost no change in this, or PDFs with refit.

Also make changes in cross-sections for dimuon data. In this case definition of separation into observable cross-section dependent on GMVFNS.

In practice χ^2 changes by at most 1 unit. Essentially no change in PDFs.

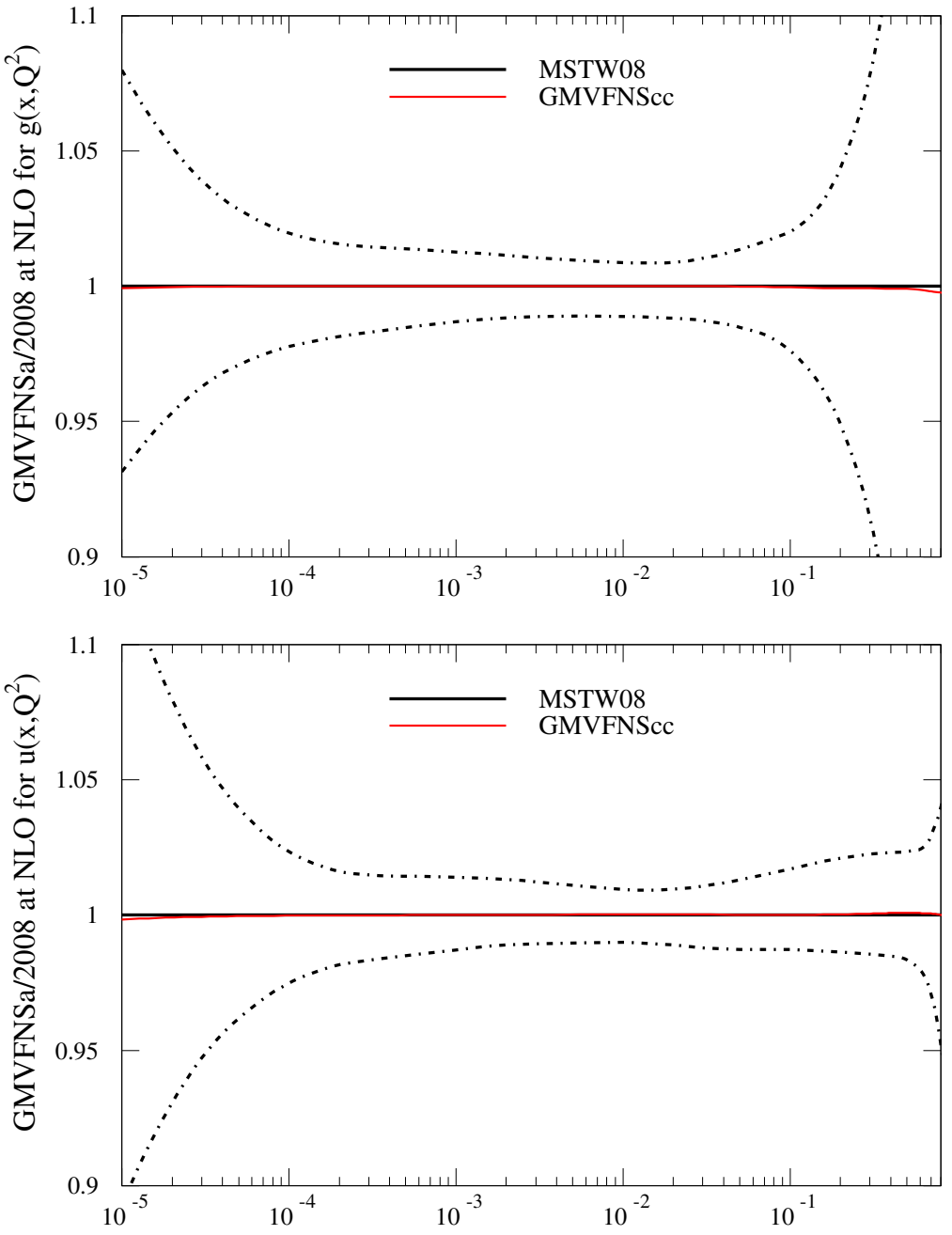

Variations in partons extracted from global fit due to different choices of GM-VFNS at NNLO.

Initial changes in $\chi^2 < 20$.

Converge to about 10. None a marked improvement.

At worst changes approach *uncertainty*.

Biggest variation in high-x gluon, which has large uncertainty.

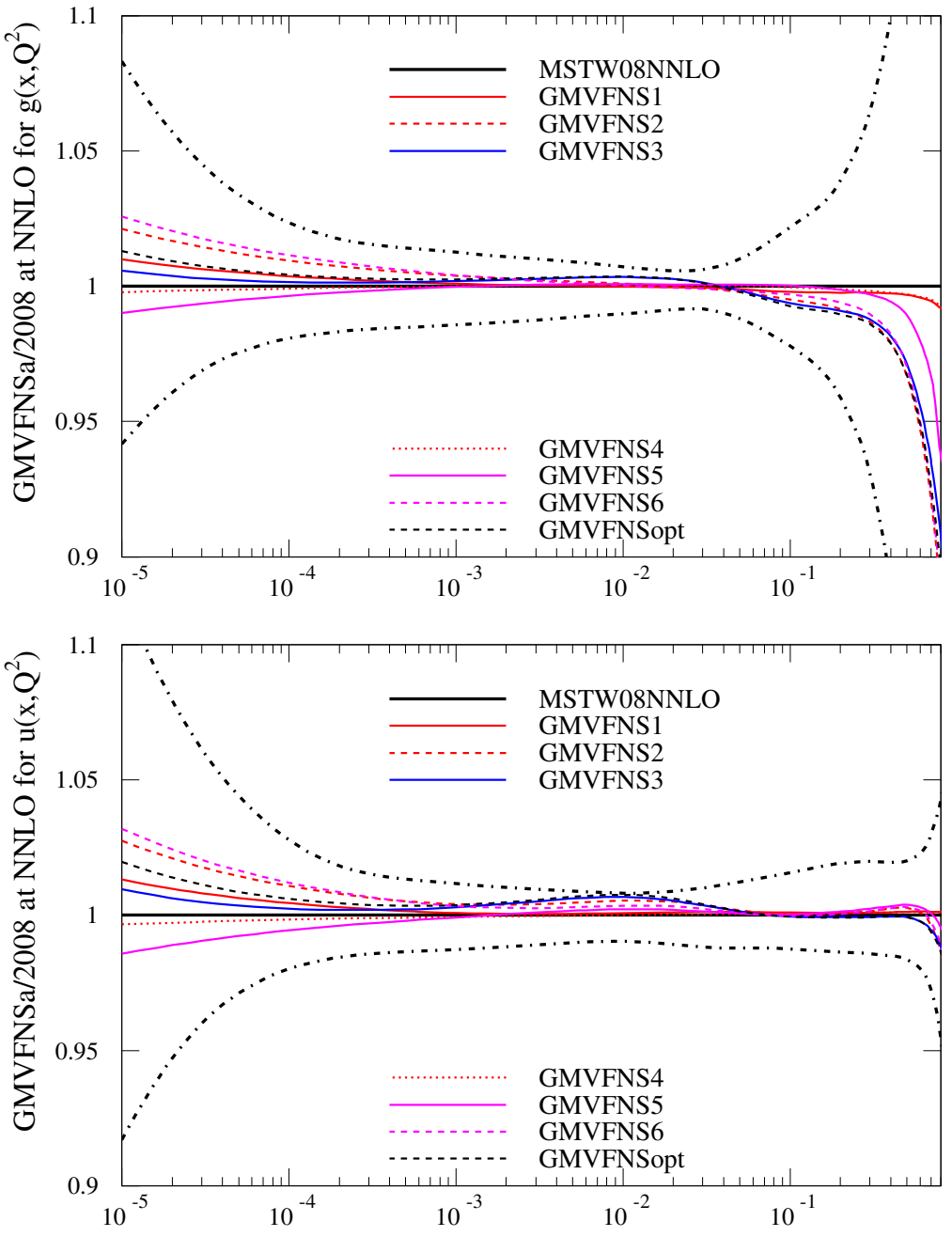

Model $\mathcal{O}(\alpha_S^3)$ at low Q^2 using known leading threshold logarithms (Laenen and Moch) and leading $\ln(1/x)$ term from k_T-dependent impact factors Catani, *et al*.

Include latter in form

$$\propto (1 - z/x_{\max})^a (\ln(1/z) - b)/z,$$

where default $a = 20, b = 4$.

Variations in a make little difference. Maximum *sensible* variation of $b = 2$ leads to effect in PDFs shown.

Major effect at smallest x.

Moderated significantly if $\mathcal{O}(\alpha_S^3)$ falls away rather than frozen.

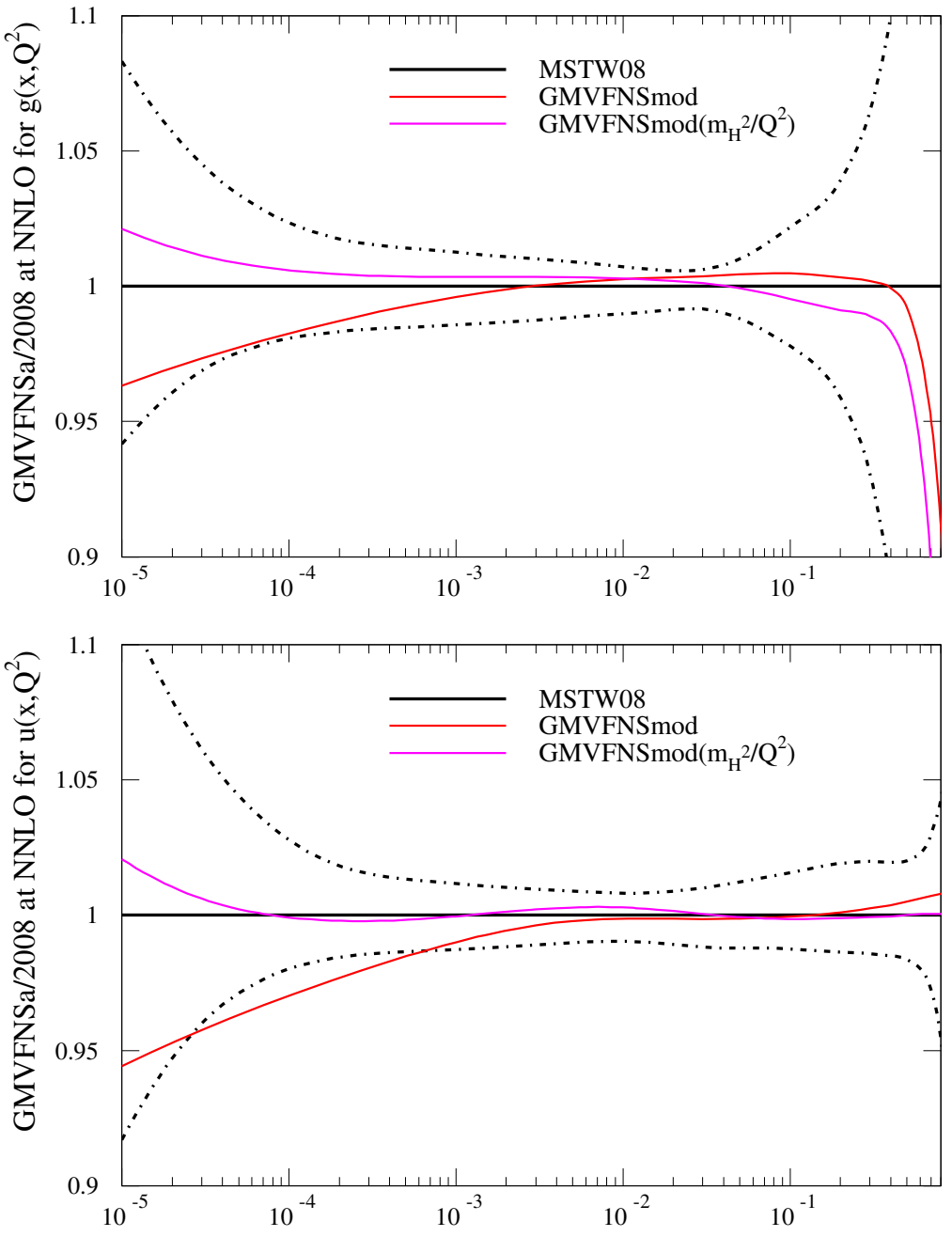

The values of the predicted cross-sections at NLO for Z and a 120 GeV Higgs boson at the Tevatron and the LHC (latter for 14 TeV centre of mass energy).

PDF set	$B_{l^+l^-}\cdot\sigma_Z$(nb) TeV	σ_H(pb)TeV	$B_{l^+l^-}\cdot\sigma_Z$(nb) LHC	σ_H(pb) LHC
MSTW08	0.2426	0.7462	2.001	40.69
GMvar1	0.2433	0.7428	2.023	40.76
GMvar2	0.2444	0.7383	2.061	41.29
GMvar3	0.2429	0.7438	2.024	41.03
GMvar4	0.2425	0.7457	1.993	40.60
GMvar5	0.2423	0.7454	1.991	40.56
GMvar6	0.2434	0.7431	2.032	41.00
GMvarcc	0.2427	0.7451	2.001	40.65

At most 1% variation at Tevatron in σ_Z.

Up to $+3\%$ and -0.5% variation in σ_Z at the LHC. About half as much in σ_H due to higher average x sampled.

Remember 8% from ZMVFNS to GMVFNS in CTEQ6 (6% for completed NNLO GMVFNS in MRST06).

The values of the predicted cross-sections at NNLO. σ_H calculated using Harlander, Kilgore code.

PDF set	$B_{l^+l^-}\cdot\sigma_Z$(nb) TeV	σ_H(pb)TeV	$B_{l^+l^-}\cdot\sigma_Z$(nb) LHC	σ_H(pb) LHC
MSTW08	0.2507	0.9550	2.051	50.51
GMvar1	0.2509	0.9505	2.054	50.39
GMvar2	0.2514	0.9478	2.061	50.55
GMvar3	0.2516	0.9539	2.062	50.88
GMvar4	0.2507	0.9534	2.050	50.45
GMvar5	0.2509	0.9519	2.046	50.37
GMvar6	0.2509	0.9462	2.057	50.38
GMvarmod	0.2501	0.9511	2.022	50.03
GMvarmod'	0.2508	0.9482	2.052	50.57

Other than from model dependence maximum variations of order 0.5% at LHC. High-x gluon leads to 1% on σ_H at Tevatron.

Model uncertainties can be $> 1\%$ from region at very small x and low Q^2. Can perhaps input more small-x knowledge here. Effect far smaller when $\mathcal{O}(\alpha_S^3)$ term falls with Q^2.

Previously noticed very slight change of slope at transition point.

Already using all variation at $Q^2 > m_h^2$

Smoothness improved at low Q^2 by slight change in model for $\mathcal{O}(\alpha_S^3)$ coefficient function.

Threshold logs plus small-x term of form

$$(1-x)^{20} * A/x(\ln(1-x) - 4) f(Q^2/m_h^2)$$

where A and $F(Q^2/m_h^2)$ known from small-x resummation (Catani *et al*).

-4 guess like approx NNLO splitting functions. Allow very slightly different Q^2-dependence in this term.

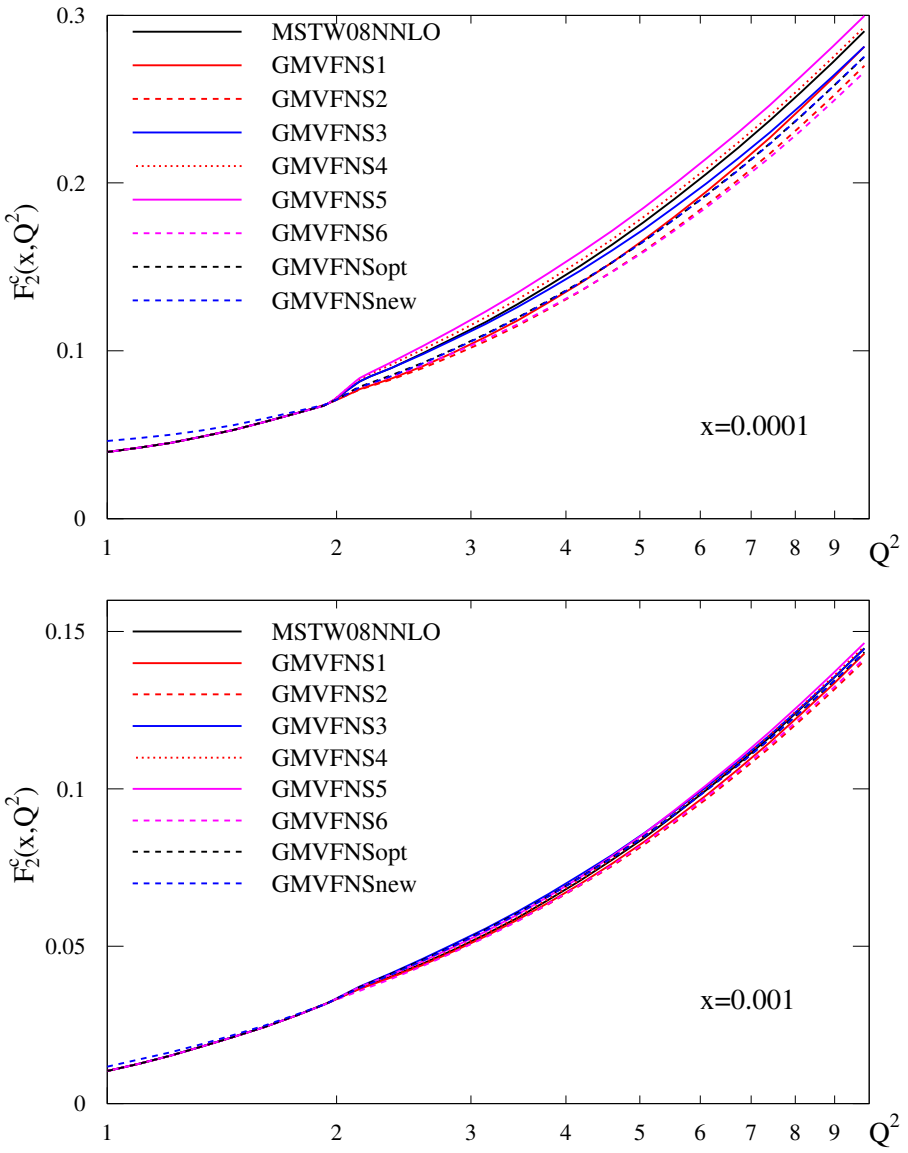

Shown as single curve in order to see more clearly.

Slight kink at very low x due to sensitivity to new $\ln(1/x)/x$ terms at NNLO.

Change leads to essentially no difference in PDFs or predictions.

Improved threshold calculations (Lo Presti *et al*), not available at time of MSTW2008. Will use in future. Rather similar effect to above. Extremely little change in fit, but slightly smoother $F_2^h(x, Q^2)$.

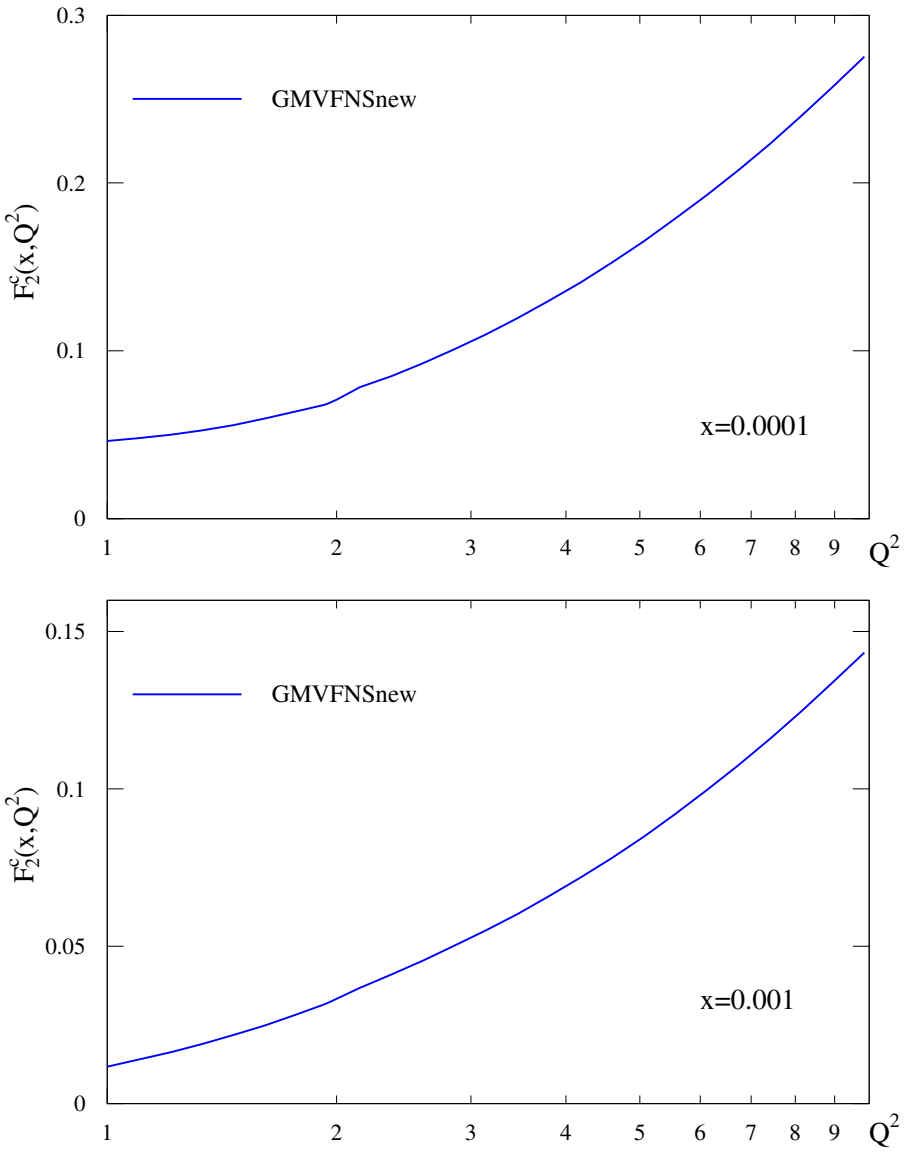

In the default scheme the best fit value at NLO turns out to be $m_c = 1.45\mathrm{GeV}$ with a very marginally better fit quality than $m_c = 1.4\mathrm{GeV}$. When m_c is allowed to vary using the optimal scheme at NLO the best fit value is for $m_c = 1.35\mathrm{GeV}$, and the quality of the fit is 6 units better than for $m_c = 1.4\mathrm{GeV}$ and 27 units better than the best fit for $m_c = 1.45\mathrm{GeV}$ using the default scheme.

The fit prefers the smoother behaviour near the transition point in the optimal scheme, but the slower turn on of F_2^c at low Q^2 results in a preference for a lower mass.

At NNLO the best fit mass is also smaller. It changes from $m_c = 1.26\mathrm{GeV}$ in the default to $m_c = 1.23\mathrm{GeV}$ using the optimal scheme. The best fit quality for the preferred mass is 7 units lower using the optimal scheme at NNLO.

Hence, the separation in the values for the pole charm mass has reduced from $0.19\mathrm{GeV}$ to $0.12\mathrm{GeV}$ using the optimum scheme, and both NLO and NNLO fits are within their uncertainty for m_c for a value of $m_c = 1.30\mathrm{GeV}$.

Conclusions

Discussed the definition of the GMVFNS, Seen change of slope and improvements in quality of fit at NNLO.

Introduced options for exact reduction to correctly ordered high and low Q^2/m_H^2 limits. New optimal version the smoothest near threshold and best fit at NLO. Little variation in smoothness or fit quality at NNLO.

Examined limits of variation in definitions and looked at variations in PDFs and cross-sections. At NLO PDFs can vary significantly outside experimental uncertainties at small x and cross-sections change by 3%. Default near extreme of variations. ZMVFNS consistently outside range of variation.

At NNLO PDFs usually (well) within uncertainties, and cross-sections rarely change more than 1%. GMVFNS variation significant source of uncertainty at NLO but much less significant at NNLO.

"Optimal" GMVFNS scheme smoothest at transition point, gives best (or very close to best) fit and less variation in extracted m_c value.

Production of $Z + b\bar{b}$ in different schemes.

In 4FS diagrams including final state bottom quarks appear at $\mathcal{O}(\alpha_S^2)$.

Explicit expressions by P.J. Rijken, W.L. van Neerven.

Last two contribute to $b\bar{b}$ quarks in the final state, and are by orders of magnitude the dominant diagrams.

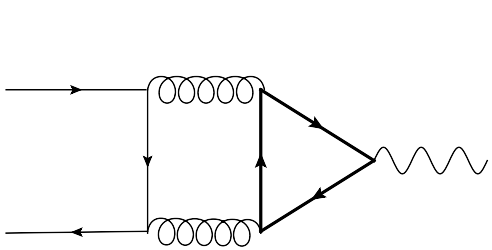

(a)

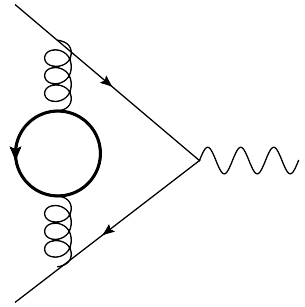

(b)

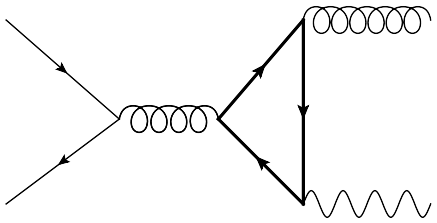

(c)

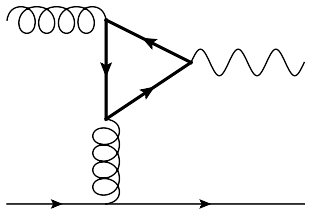

(d)

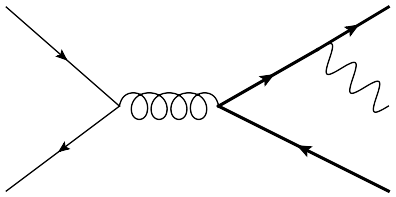

(e)

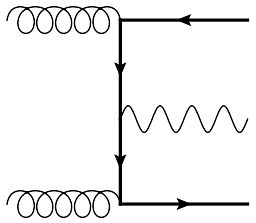

(f)

subprocess	Tevatron	LHC, 7 TeV	LHC, 14 TeV
$q + \bar{q} \to Z$	5.230×10^{-6}	-2.124×10^{-5}	-6.440×10^{-5}
$q + \bar{q} \to Z + g$	4.901×10^{-5}	6.185×10^{-5}	9.701×10^{-5}
$q(\bar{q}) + g \to Z + q(\bar{q})$	-2.862×10^{-5}	-1.456×10^{-4}	-2.632×10^{-4}
$q + \bar{q} \to Z + b + \bar{b}$	3.754×10^{-4}	1.450×10^{-3}	3.382×10^{-3}
$g + g \to Z + b + \bar{b}$	2.090×10^{-4}	5.287×10^{-3}	1.997×10^{-2}
total	6.100×10^{-4}	6.632×10^{-3}	2.312×10^{-2}

Additional $\mathcal{O}(\alpha_S^2)$ contributions to the total Z 4FS NNLO cross section in nb (multiplied by leptonic branching ratio) at the Tevatron and LHC arising from real and virtual b-quark processes.

Clearly the $g \to b\bar{b}$ initiated process is very dominant at the LHC.

Tevatron, 1.96 TeV	$B \cdot \sigma^Z_{\rm NLO}(4{\rm FS})$	$B \cdot \sigma^Z_{\rm NLO}(5{\rm FS})$	$B \cdot \sigma^Z_{\rm NLO}(5{\rm FS}, b)$
σ^Z_0	0.1989	0.1990	0.0012
σ^Z_1	0.0413	0.0436	-0.0002
total	0.2402	0.2426	0.0010

LHC, 7 TeV	$B \cdot \sigma^Z_{\rm NLO}(4{\rm FS})$	$B \cdot \sigma^Z_{\rm NLO}(5{\rm FS})$	$B \cdot \sigma^Z_{\rm NLO}(5{\rm FS}, b)$
σ^Z_0	0.7846	0.8023	0.0205
σ^Z_1	0.1206	0.1285	-0.0020
total	0.9052	0.9308	0.0185

LHC, 14 TeV	$B \cdot \sigma^Z_{\rm NLO}(4{\rm FS})$	$B \cdot \sigma^Z_{\rm NLO}(5{\rm FS})$	$B \cdot \sigma^Z_{\rm NLO}(5{\rm FS}, b)$
σ^Z_0	1.6922	1.7545	0.0656
σ^Z_1	0.2303	0.2465	-0.0050
total	1.9225	2.0009	0.0601

NLO predictions for the Z cross section (in nb), multiplied by leptonic branching ratio, at the Tevatron and LHC using MSTW 2008 NLO PDF, broken down into α_S^n ($n = 0, 1$) contributions, in the 4FS and 5FS calculation. The final column gives the contribution in the 5FS from processes where the Z couples directly to b quarks.

Tevatron, 1.96 TeV	$B \cdot \sigma^Z_{\rm NNLO}(\rm 4FS)$	$B \cdot \sigma^Z_{\rm NNLO}(\rm 5FS)$	$B \cdot \sigma^Z_{\rm NNLO}(\rm 5FS, b)$
σ^Z_0	0.2013	0.2016	0.0012
σ^Z_1	0.0409	0.0431	-0.0002
σ^Z_2	0.0063	0.0060	-0.0003
total	0.2485	0.2507	**0.0008**
$\Delta_b \sigma^Z$	**0.0006**	–	
total + $\Delta_b \sigma^Z$	0.2491	0.2507	

NNLO predictions for the total Z cross section (in nb), multiplied by leptonic branching ratio at the Tevatron using MSTW 2008 NNLO PDFs as input, broken down into the α_S^n $(n = 0, 1, 2)$ contributions. The final column gives the contribution to the 5FS cross sections from processes where the Z couples directly to b quarks. The additional $\mathcal{O}(\alpha_S^2)$ contributions to the cross section arising from real and virtual b-quark processes are added to the 4FS cross section in the last line.

Good overall agreement.

LHC, 7 TeV	$B \cdot \sigma^Z_{\rm NNLO}(\rm 4FS)$	$B \cdot \sigma^Z_{\rm NNLO}(\rm 5FS)$	$B \cdot \sigma^Z_{\rm NNLO}(\rm 5FS, b)$
σ^Z_0	0.8083	0.8266	0.0202
σ^Z_1	0.1239	0.1322	-0.0020
σ^Z_2	0.0037	-0.0002	-0.0037
total	0.9359	0.9586	**0.0145**
$\Delta_b \sigma^Z$	**0.0066**	–	
total + $\Delta_b \sigma^Z$	0.9426	0.9586	

NNLO predictions for the total Z cross section (in nb), multiplied by leptonic branching ratio at the LHC (7TeV) using MSTW 2008 NNLO PDFs as input, broken down into the α_S^n ($n = 0, 1, 2$) contributions. The final column gives the contribution to the 5FS cross sections from processes where the Z couples directly to b quarks. The additional $\mathcal{O}(\alpha_S^2)$ contributions to the cross section arising from real and virtual b-quark processes are added to the 4FS cross section in the last line of each sub-table.

Pretty good agreement for light flavours, but 5FS more than twice 4FS for b contribution.

LHC, 14 TeV	$B \cdot \sigma^Z_{\rm NNLO}(\rm 4FS)$	$B \cdot \sigma^Z_{\rm NNLO}(\rm 5FS)$	$B \cdot \sigma^Z_{\rm NNLO}(\rm 5FS, b)$
σ^Z_0	1.7472	1.8110	0.0641
σ^Z_1	0.2384	0.2557	-0.0050
σ^Z_2	-0.0047	-0.0153	-0.0107
total	1.9809	2.0514	**0.0484**
$\Delta_b \sigma^Z$	**0.0231**	–	
total + $\Delta_b \sigma^Z$	2.0040	2.0514	

NNLO predictions for the total Z cross section (in nb), multiplied by leptonic branching ratio at the LHC (14TeV) using MSTW 2008 NNLO PDFs as input, broken down into the α_S^n $(n = 0, 1, 2)$ contributions. The final column gives the contribution to the 5FS cross sections from processes where the Z couples directly to b quarks. The additional $\mathcal{O}(\alpha_S^2)$ contributions to the cross section arising from real and virtual b-quark processes are added to the 4FS cross section in the last line of each sub-table.

Pretty good agreement for light flavours, but 5FS twice 4FS for b contribution.

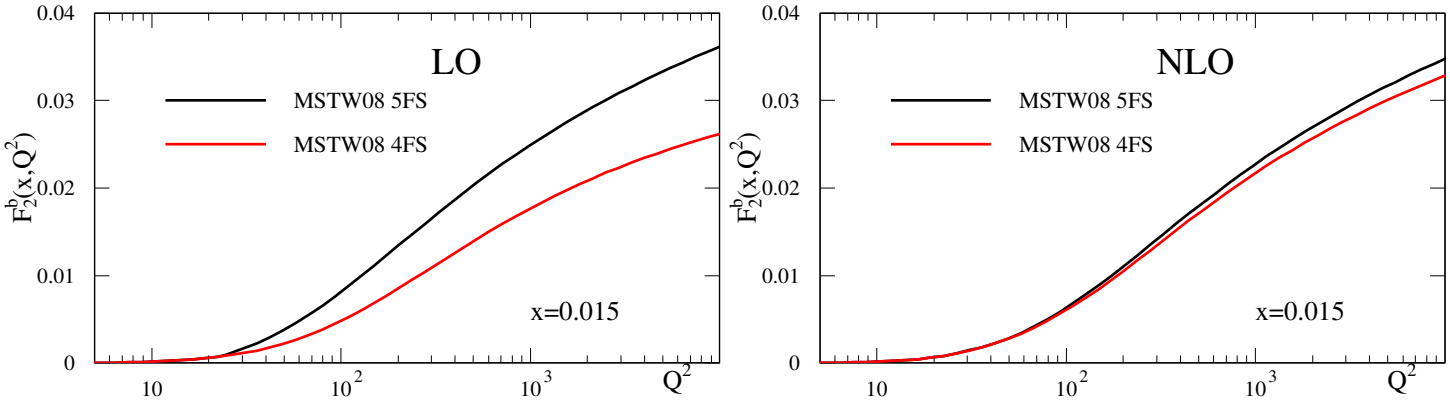

At LO for relevant $x \sim 0.015$ the lack of resummation in 4FS leads to the structure function (driven mainly by $g \to b\bar{b}$) being suppressed to only $\sim 70\%$ of 5FS result. This should be squared in hadron-hadron process, hence factor of ~ 2.

At NLO double log corrects most of this, only $\sim 90\%$ suppression in structure functions.

However, only one of the incoming gluons has double-log correction in hadron-hadron process at NLO ($\mathcal{O}(\alpha_S^3)$). Expect correction factor of about 1.5 at NLO.

Cross Section	$m_b \neq 0$ (pb) [ratio]	$m_b = 0$ (pb) [ratio]
σ^{LO}	2.21[–]	2.37[–]
σ^{NLO} *inclusive*	3.40[1.54]	3.64[1.54]
σ^{NLO} *exclusive*	2.80[1.27]	3.01[1.27]

Indeed, much as seen in recent Febres Cordero, Reina and Wackeroth calculation.

4FS still about 70% that of 5FS calculation.

Slower convergence of 4FS calculations in hadron-hadron processes. Similar results seen for Higgs cross-sections.